Superconducting transition temperature of Pb nanofilms: Impact of thickness-dependent oscillations of the phonon-mediated electron-electron coupling

Yajiang Chen, A. A. Shanenko, and F. M. Peeters*
Departement Fysica, Universiteit Antwerpen, Groenenborgerlaan 171, B-2020 Antwerpen, Belgium
(Received 5 December 2011; revised manuscript received 20 April 2012; published 14 June 2012)

To date, several experimental groups reported measurements of the thickness dependence of T_c of atomically uniform single-crystalline Pb nanofilms. The reported amplitude of the T_c oscillations varies significantly from one experiment to another. Here we propose that the reason for this unresolved issue is an interplay of the quantum-size variations in the single-electron density of states with thickness-dependent oscillations in the phonon-mediated electron-electron coupling. Such oscillations in the coupling depend on the substrate material, the quality of the interface, the protection cover, and other details of the fabrication process, changing from one experiment to another. This explains why the available data do not exhibit one-voice consistency about the amplitude of the T_c oscillations. Our analyses are based on a numerical solution of the Bogoliubov-de Gennes equations for a superconducting slab.

DOI: 10.1103/PhysRevB.85.224517 PACS number(s): 74.78.Na

I. INTRODUCTION

Quantum-size effects on the excitation gap[1,2] and the transition temperature[4–6] in superconducting ultrathin films have been a subject of study since Blatt and Thompson in 1963 predicted that the superconducting gap in ultrathin films oscillates as a function of the thickness.[1] Such oscillations are caused by the quantization of the electron motion in the direction normal to the film. In particular, the formation of discrete electron levels [i.e., the quantum well states (QWS)][7,8] splits the three-dimensional (3D) conduction band into a series of two-dimensional (2D) subbands. The bottom of each subband is at the energy position of the corresponding QWS and so it is shifted down (up) when increasing (decreasing) the nanofilm thickness. When one of the QWS approaches the Fermi level, the density of the single-electron states at the Fermi level $N(0)$ increases, resulting in enhanced superconductivity.

Recently, superconducting Pb nanofilms have been intensively investigated experimentally where electronic effects are much stronger than effects due to strain. The critical temperature of atomically flat Pb nanofilms with thickness down to a few monolayers on a Si(111) substrate have been measured under different conditions.[3–6,8–10] It was found that superconductivity is not destroyed by fluctuations even when the thickness of the nanofilm is only a single monolayer,[10] and the dependence of the critical temperature on thickness shows oscillations with a period close to two monolayers (ML)[3,5] (i.e., the even-odd staggering in the superconducting properties).

In addition to $N(0)$, the phonon-mediated coupling g between electrons also makes an important contribution to superconductivity. Large efforts[11–14] have been made to understand how the formation of QWS can affect the electron mass-enhancement factor $\lambda \sim gN(0)$ [only in the weak-coupling limit $\lambda = gN(0)$]. Experimentally, from the information of the temperature dependence of the line widths of QWS in Ag films deposited on top of Fe(111) whisker, it was found that λ exhibits an overall decrease with increasing film thickness so that λ approaches its bulk value as $\approx 1/N$, where N is the number of monolayers.[11] The experimental study of λ in Pb(111) nanofilms on silicon showed that the mass-enhancement factor increases with increasing N. In both cases λ exhibits pronounced thickness-dependent oscillations. As it is mentioned above, a well-known reason for these oscillations is the variation of $N(0)$ with the nanofilm thickness. However, this is not the only important reason. There is an additional (less known) effect coming from thickness-dependent oscillations of the coupling g. The interplay of the oscillations of g and $N(0)$ is not well understood yet and often overlooked. In our previous paper[2] we initiated a study of such an interplay based on intuitive arguments and used an ansatz for the thickness dependent g. In the present paper we revisit the problem and develop a simple model to justify this ansatz and to analyze all the currently available experimental data of T_c versus film thickness. Our investigation is based on a numerical solution of the Bogoliubov-de Gennes (BdG) equations. However, instead of solving the full BdG formalism,[2] we make use of the Anderson recipe for a very accurate approximate semianalytical solution to the BdG equations: Corrections to the Anderson approximation are less than a few percent for nanofilms. This will significantly simplify our numerical analysis.

Our paper is organized as follows. In Sec. II we outline the BdG equations for a superconducting slab, including the basic moments concerning the Anderson approximation. In Sec. III we discuss our numerical results on the critical temperature in ultrathin superconducting nanofilms and highlight important aspects due to the interplay of the thickness-dependent oscillations of $N(0)$ and g. We demonstrate that this interplay is responsible for significant variations in the amplitude of the quantum-size oscillations of T_c from one experiment to another. Our conclusions are given in Sec. IV.

II. FORMALISM

A. Bogolibov-de Gennes equations for a superconducting slab

The translational invariance is broken in the presence of quantum confinement so that the superconducting order parameter Δ becomes position dependent in nanoscale superconductors [i.e., $\Delta = \Delta(\mathbf{r})$]. In this case the profile of $\Delta(\mathbf{r})$ can be found from the BdG equations (see the textbook[16]) which

are written as (for zero magnetic field)

$$\begin{bmatrix} \hat{H}_e & \Delta(\mathbf{r}) \\ \Delta(\mathbf{r}) & -\hat{H}_e \end{bmatrix} \begin{bmatrix} u_{i\mathbf{k}}(\mathbf{r}) \\ v_{i\mathbf{k}}(\mathbf{r}) \end{bmatrix} = E_{ik} \begin{bmatrix} u_{i\mathbf{k}}(\mathbf{r}) \\ v_{i\mathbf{k}}(\mathbf{r}) \end{bmatrix}, \tag{1}$$

where $\hat{H}_e = -\frac{\hbar^2}{2m_e}\nabla^2 - \mu$ is the single-electron Hamiltonian (for zero magnetic field) measured from the chemical potential μ; i is the quantum number associated with QWS for electron motion in the z direction perpendicular to the film, and $\mathbf{k} = (k_x, k_y)$ is the wave vector for quasifree motion of electrons parallel to the film ($k = |\mathbf{k}|$); $u_{i\mathbf{k}}(\mathbf{r})$ and $v_{i\mathbf{k}}(\mathbf{r})$ are the particle- and holelike wave functions; E_{ik} stands for the quasiparticle energy; and $\Delta(\mathbf{r})$ is the superconducting order parameter (chosen as real). The BdG equations are solved in a self-consistent manner with the self-consistency condition given by[16]

$$\Delta(\mathbf{r}) = g \sum_{i\mathbf{k}} u_{i\mathbf{k}}(\mathbf{r}) v^*_{i\mathbf{k}}(\mathbf{r}) \tanh(\beta E_{ik}/2), \tag{2}$$

where $g > 0$ is the effective coupling of electrons and $\beta = 1/(k_B T)$. The summation in Eq. (2) runs over states with the single-electron energy ξ_{ik} inside the Debye window (i.e., $|\xi_{ik}| < \hbar\omega_D$) with $\hbar\omega_D = 8.27$ meV for Pb (see the textbooks[16,17]).

As known, the BdG equations can, in principle, be solved without additional approximations. However, even for ultrathin nanofilms this can be a time-consuming task, especially in the vicinity of T_c, where a large number of iterations is usually needed for a proper convergence. This is why it is useful to invoke Anderson's recipe for a semianalytical approximate solution. The use of Anderson's recipe is well justified because (i) corrections were found to be less than a few percent for nanofilms (see, e.g., Ref. 15) and (ii) resulting equations are much easier for numerical implementation. In terms of the particle- and holelike amplitudes, the Anderson approximation reads

$$u_{i\mathbf{k}}(\mathbf{r}) = \mathcal{U}_{ik}\psi_{i\mathbf{k}}(\mathbf{r}), \quad v_{i\mathbf{k}}(\mathbf{r}) = \mathcal{V}_{ik}\psi_{i\mathbf{k}}(\mathbf{r}), \tag{3}$$

where $\mathcal{U}_{ik}$ and $\mathcal{V}_{ik}$ are multiplicative factors (real) and $\psi_{i\mathbf{k}}(\mathbf{r})$ is the single-electron wave function [i.e., $\hat{H}_e\psi_{i\mathbf{k}}(\mathbf{r}) = \xi_{ik}\psi_{i\mathbf{k}}(\mathbf{r})$]. In the case of interest (i.e., for a superconducting slab), we have

$$\psi_{i\mathbf{k}}(\mathbf{r}) = \frac{\varphi_i(z)}{\sqrt{L_x L_y}} e^{i(k_x x + k_y y)}, \tag{4}$$

where $\varphi_i(z)$ is the QWS wave function and L_x, L_y are the dimensions of the unit cell used for the periodic boundary conditions in the x and y directions. For infinite confinement of electrons in the slab with thickness d ($L_x, L_y \gg d$) we have $\varphi_i(z) = \sqrt{2/d}\sin(\pi(i+1)z/d)$ and

$$\xi_{ik} = \frac{\hbar^2}{2m_e}\left[\frac{\pi^2(i+1)^2}{d^2} + k^2\right] - \mu. \tag{5}$$

Inserting Eq. (3) into Eq. (1) and introducing the subband-dependent gap [in the case of interest $\Delta(\mathbf{r}) = \Delta(z)$],

$$\Delta_i = \int dz\, \varphi_i^2(z)\Delta(z), \tag{6}$$

we find a homogeneous system of two linear equations controlling $\mathcal{U}_{ik}$ and $\mathcal{V}_{ik}$. The determinant of the corresponding matrix should be equal to zero for a nontrivial solution, leading to $E_{ik} = \sqrt{\xi_{ik}^2 + \Delta_i^2}$. Then, by using the standard normalization condition $\mathcal{U}_{ik}^2 + \mathcal{V}_{ik}^2 = 1$, the BdG equations are reduced to the BCS-like self-consistency equation:

$$\Delta_{i'} = \frac{1}{2}\int \frac{d^2k}{(2\pi)^2} \sum_i \Phi_{i'i} \frac{\Delta_i}{E_{ik}} \tanh(\beta E_{ik}/2), \tag{7}$$

with the interaction-matrix element,

$$\Phi_{i'i} = g \int dz\, \varphi_{i'}^2(z)\varphi_i^2(z). \tag{8}$$

As T approaches the critical temperature T_c, E_{ik} reduces to the single-electron energy ξ_{ik} independent of Δ_i. Hence, at T_c Eq. (7) becomes a linear homogeneous system of equations for Δ_i that has a nontrivial solution when the corresponding determinant is zero, that is,

$$\det[M_{i'i} - \delta_{i'i}] = 0, \tag{9}$$

from which we obtain T_c. In Eq. (9),

$$M_{i'i} = \frac{m_e}{2\pi\hbar^2}\int_{-\hbar\omega_D}^{\hbar\omega_D} d\xi\ \theta(\xi - \varepsilon_i)\frac{\Phi_{ii'}}{2|\xi|}\tanh(\beta_c|\xi|/2), \tag{10}$$

with $\beta_c = 1/(k_B T_c)$ and $\varepsilon_i = \frac{\hbar^2}{2m_e}\frac{\pi^2(i+1)^2}{d^2} - \mu$. We note that a numerical solution of Eq. (9) is significantly faster than the procedure based on a numerical study of the BdG equations. The point is that Eq. (9) yields directly the value of T_c. In contrast, to calculate T_c from the BdG equations, one first needs to find Δ_i as function of temperature. Then, T_c can be extracted from these data as the temperature above for which there exists only zero solution for Δ_i. In addition, such a BdG-based numerical procedure of determining T_c is rather capricious in practice because at temperatures close to T_c convergence becomes rather slow and it is difficult to estimate an appropriate number of iterations to approach a solution. This often results in an overestimation of T_c that is larger than the corrections to the Anderson approximation (i.e., one more solid argument in favor of the present numerical scheme).

B. Quantum-size variations of the electron-electron coupling

In Sec. II A it is assumed that the phonon-mediated coupling of electrons g is not position dependent. It is true for bulk and a good approximation even for metallic nanofilms with thickness $d \gtrsim$ 10–20 nm (see our results below). However, this is not the case for ultrathin nanofilms due to significantly different (as compared to bulk) conditions for the lattice vibrations at the interface between the film and the semiconductor substrate. As we are interested in superconducting quantum-size oscillations typical for ultrathin metallic films, the question arises how our formalism should be modified to take account of this feature.

The coupling between electrons will depend on the proximity to the interface [i.e., $g = g(z)$]. Deep in the film, $g(z)$ approaches the bulk coupling g_0. For Pb we take[16,17] $g_0 N_{\text{bulk}}(0) = 0.39$, with $N_{\text{bulk}}(0)$ the bulk density of states at the Fermi energy. Approaching the interface, $g(z)$ is not equal to g_0 any longer but acquires a different value g_{if}. Therefore,

to first approximation we can replace $g(z)$ by the step function,

$$g(z) = \begin{cases} g_{\rm if} & 0 \leqslant z \leqslant d_{\rm if}, \\ g_0 & d_{\rm if} < z \leqslant d, \end{cases} \tag{11}$$

where $d_{\rm if}$ can be interpreted as the interface thickness. When introducing the spatial dependence of the coupling between electrons, Eq. (8) is replaced by

$$\Phi_{i'i} = \int dz\, g(z)\, \varphi_{i'}^2(z)\varphi_i^2(z), \tag{12}$$

so that we obtain

$$\Phi_{i'i} \approx \frac{\bar{g}}{d}(1+\delta_{i'i}), \quad \bar{g} \approx \frac{1}{d}\int_0^d dz g(z). \tag{13}$$

As seen, to take into account the interface effect on the electron-electron effective coupling, one should replace g in all the relevant formulas in Sec. II A by its spatially averaged value $\bar{g}$ given by Eq. (14). Based on Eqs. (11) and (14), we can find

$$\bar{g} = g_0 - \frac{d_{\rm if}(g_0 - g_{\rm if})}{aN}, \tag{14}$$

where a is the lattice constant in the direction of the film growth and N is the number of monolayers in the film [$d = aN$, and we take $a = 0.286$ Å for Pb(111); see Ref. 12]. As seen from Eq. (14), the presence of the interface results in an extra contribution to $\bar{g}$ decaying with increasing thickness as $1/N$. This is typical of the surface effects whose relative contribution can be estimated as roughly proportional to the ratio of the whole surface area to the system volume. Such a contribution to the coupling was first reported in Ref. 11, where the electron-phonon mass enhancement parameter λ in Ag films grown on top of Fe(100) was experimentally studied and found to be dependent on the film thickness. As known, $\lambda = gN(0)$ for $g \to 0$, with $N(0)$ the density of states, and λ is often called the (dimensionless) coupling constant. *Ab initio* DFT calculations of λ also revealed the presence of the $1/N$ contribution (see, e.g., Refs. 11 and 14). Note that the well-known softening of the phonon modes due to surface effects (see, e.g., Ref. 18) can be incorporated in a similar manner. Below we assume that all surface effects are included in $g_{\rm if}$. The same holds for effects due to a protective cover.

While g_0 is the film-material constant, $g_{\rm if}$ is not and changes from one experiment to another. Moreover, $g_{\rm if}$ varies also with changing nanofilm thickness because of quantum-size oscillations in the interface properties; see, for instance, theoretical results and discussion about the surface energy and the work function in nanofilms.[12] Generally, the quantum-size oscillations are controlled by a multiple-subband structure appearing in the single-electron spectrum due to the formation of QWS. Each time when the bottom of a subband (QWS) crosses μ, a shape (quantum-size) resonance appears[1] with a significant effect on the system characteristics. From Eq. (5) it is clear that the shape resonances are periodic with period half the Fermi wavelength $\lambda_F/2$. Thus, assuming that $g_{\rm if}$ exhibits thickness-dependent oscillations with period $\lambda_F/2$, Eq. (14) can be represented in the form,

$$\bar{g} = g_0 - \frac{g_1(4\pi aN/\lambda_F)}{N}, \tag{15}$$

where $g_1(x)$ is a periodic function with $g_1(0) = g_1(2\pi)$. Below, in our numerical study of the BdG equations, we replace g in the formulas of Sec. II A by $\bar{g}$ given by Eq. (15).

It is worth noting that one should distinguish oscillations of g from those of the electron-phonon mass enhancement parameter λ. As $\lambda \approx gN(0)$, there are two sources of quantum-size oscillations in λ [i.e., (i) the density of states that exhibits an increase each time when a new QWS crosses μ, and (ii) the phonon-mediated coupling g]. The oscillations of λ are a known point that was investigated previously in experiments and in theoretical studies (see, e.g., Refs. 11–14). However, effects of the interplay of oscillations of $N(0)$ with those of g were not investigated and reported.

Experimentally measured values of the period of the quantum-size oscillations in Pb nanofilms are found to be very close to 2 ML. However, the period is not exactly 2 ML so that the even-odd staggering in the basic superconducting properties has phase-slip points where the phase of the even-odd oscillations changes by π. When $4a/\lambda_F = 1$, i.e., the period is equal to 2 ML, then we deal only with two parameters $g_1(\pi)$ and $g_1(2\pi)$ because $g_1(4\pi aN/\lambda_F)$ is equal to $g_1(\pi)$ for an odd number of monolayers and to $g_1(2\pi)$ for an even number of monolayers. On the contrary, when $4a/\lambda_F$ is not an integer, we need to go into more detail about the dependence of g_1 on N. There is the possibility of overcoming this problem by using, say, a "minimal scenario" when choosing the chemical potential such that the period of the quantum-size oscillations is exactly 2 ML. In this case we are able to limit ourselves to only two fitting parameters $g_1(\pi)$ and $g_1(2\pi)$. Therefore, our theoretical analysis will be restricted to the data between the phase-slip points where the effects of the mismatch between $0.5\lambda_F$ and 2 ML can be neglected. Within such a minimal scenario, the parabolic band approximation used in Eq. (5) dictates that $\mu = 1.150$ eV. It corresponds to λ_F being four times the single monolayer thickness a (i.e., $\lambda_F = 1.14$ nm).

Now, we have everything at our disposal to check if the interplay between thickness-dependent oscillations of $N(0)$ and g can provide a solid understanding of the significant variations in the amplitude of the quantum-size oscillations of T_c found in different experiments.

III. RESULTS AND DISCUSSIONS

A. Brief review of experimental results on the T_c oscillations

In Fig. 1 we show all reported sets of recent experimental data on the thickness dependence of T_c in ultrathin Pb(111) nanofilms on silicon. The data indicated by circles are from Ref. 3 and were obtained by *ex situ* resistivity measurements. Here Pb nanofilms were deposited on a Si(111) substrate [with the Si(111) (7×7) reconstruction] and covered by a protective Au layer with thickness 4 ML. This set of data exhibits clear even-odd quantum-size staggering for thicknesses of 22–28 ML. For smaller thicknesses there are only data for an odd number of atomic layers (i.e., $N = 15$, 17, 19, and 21). A clear phase slip of π in the even-odd oscillations can be observed at $N = 22$ ML. At this point the even-odd staggering in T_c changes its trend: above the thickness $N = 22$ ML the critical temperature increases when passing from an odd number of monolayers to an even number, however, it decreases from

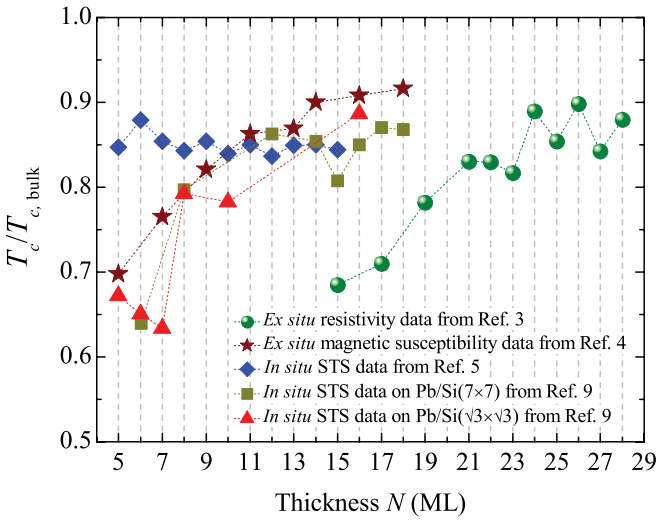

FIG. 1. (Color online) Experimental data on the thickness dependence of the critical temperature T_c of Pb nanofilms on Si(111) from different experiments.

$N = 21$ ML to $N = 22$ ML. Below we will limit the analysis of this data set to $N \geqslant 23$.

The results of Ref. 4 are given by stars and obtained from *ex situ* magnetic-susceptibility measurements for Pb films on Si(111) with the interface Si(111)$(\sqrt{3} \times \sqrt{3})$. The samples were protected by a Ge cap. The set includes data for films with an odd number of atomic layers $N = 5, 7, 9, 11, 13$ and with even numbers $N = 14, 16$, and 18. Here it is not possible to obtain significant information about the even-odd oscillations of T_c: We can only compare the data for $N = 13$ and $N = 14$. As seen from this comparison, the increase of T_c from $N = 13$ to $N = 14$ is about two times smaller than the averaged amplitude of the even-odd oscillations observed in the previous set of data from Ref. 3.

The third experimental set of thickness-dependent T_c (rhombuses; Ref. 5) is for Pb nanofilms on the substrate Si(111)(7×7). Here the data were measured by *in situ* scanning tunneling spectroscopy. There was no protective layer covering the Pb film in this case. Clear signatures of even-odd quantum-size oscillations are visible down to thickness of 5 ML. However, the amplitude of these oscillations is about 2–3 times smaller than that of the first data set.[3] It is worth noting that T_c of the third data set does not show an overall decrease with decreasing film thickness. It is seen that there are two points where the phase of the even-odd staggering of T_c slips by π (i.e., at $N = 6$ and at $N = 14$). For this set of data we will focus on the domain $7 \leqslant N \leqslant 13$.

The fourth (squares) and fifth (triangles) data sets are from the same group[9] and were measured by *in situ* scanning tunneling spectroscopy. They correspond to Pb nanofilms on a Si(111) substrate with reconstruction Si(111)(7×7) and Si(111)$(\sqrt{3} \times \sqrt{3})$, respectively. The fourth set shows the even-odd staggering of T_c for $N = 14$–18. However, here the slip point is situated at $N = 16$, which significantly reduces the number of points available for our analysis (below we work with data for $N \leqslant 15$). The fifth experimental set for T_c does not provide us with a clear pattern of even-odd oscillations. Only from the data for film thicknesses $N = 5$, 6, and 7 we can guess that the amplitude of such oscillations is not pronounced. The phase-slip point of the even-odd staggering is visible at $N = 6$ (below we make a numerical fit to the data for $N \geqslant 7$). We note that the data of the fourth set are in significant variance with those of the third set in spite of the fact that the type of measurement and the substrate-film interface were similar in both experiments.

B. Impact of the thickness-dependent coupling between electrons

Results of our numerical analysis (open symbols) are given versus the experimental data (solid symbols) in Fig. 2. In Fig. 2(a) we compare our data with the T_c values from the first set (Ref. 3). Here we choose the range $N = 23$–28 (i.e., above $N = 22$), the experimental phase-slip point of the even-odd oscillations in T_c (see the discussion in the previous section). Our calculations have been performed for $g_1(\pi) = 1.67 g_0$ (odd numbers) and $g_1(2\pi) = 2.13 g_0$ (even numbers), which yields good agreement with experiment. At first sight these values of g_1 seem too large to produce a deviation of only about 10%–20% from bulk. However, g_1/N is the correction to the electron-electron coupling rather than g_1. In particular, for $N = 20$ we obtain $g_1/N = 0.084 g_0$ for odd numbers and $g_1/N = 0.11 g_0$ for even numbers. It is worth noting that g_1 is larger for even numbers and so the resulting coupling $g_0 - g_1/N$ is smaller. However, T_c is generally larger for even numbers as compared to that for odd numbers in Fig. 1(a). The reason for this counterintuitive behavior is that there is an essential interplay between the even-odd oscillations in the density of states $N(0)$ and similar oscillations in the coupling g. In the case of Fig. 2(a) the drop in g for even N is fully overcome by an increase in $N(0)$ so that the product $gN(0)$ $[T_c \sim e^{1/(-gN(0))}]$ slightly increases for even-number films and decreases for odd-number films.

Figure 2(b) shows our theoretical results versus the experimental data of the second set from Ref. 4. Here we used the fitting parameters $g_1(\pi) = 0.64 g_0$ (for odd numbers) and $g_1(2\pi) = 1.46 g_0$ (for even numbers). As seen, g_1 for odd numbers is three times smaller than for even numbers but T_c does not exhibit any pronounced even-odd staggering. The explanation is again the interplay of the quantum-size variations of $N(0)$ with thickness-dependent oscillations in g: The effect of the difference between $g_1(\pi)$ and $g_1(2\pi)$ is almost compensated due to significant drops of $N(0)$ for even numbers of atomic layers. It is worth noting the surprisingly good agreement over the full range of experimental data.

Now we switch to the analysis of the third set of experimental data for T_c from Ref. 5. These data are compared with our theoretical results in Fig. 2(c) for $N = 7$ ML to $N = 13$ ML (i.e., between the two phase-slip points $N = 6$ and $N = 14$). For this data set T_c does not exhibit an overall decrease with decreasing N but oscillates around a value that is about 15% lower than the bulk critical temperature of 7.2 K. Even for $N = 50$ ML the critical temperature was found to be about 15% smaller than in bulk. The bulk value of T_c and the superconducting energy gap were achieved only for relatively thick films with $N = 500$ ML. To incorporate this feature, we introduce a slightly smaller effective electron-phonon coupling constant g_{eff} which replaces the bulk coupling constant

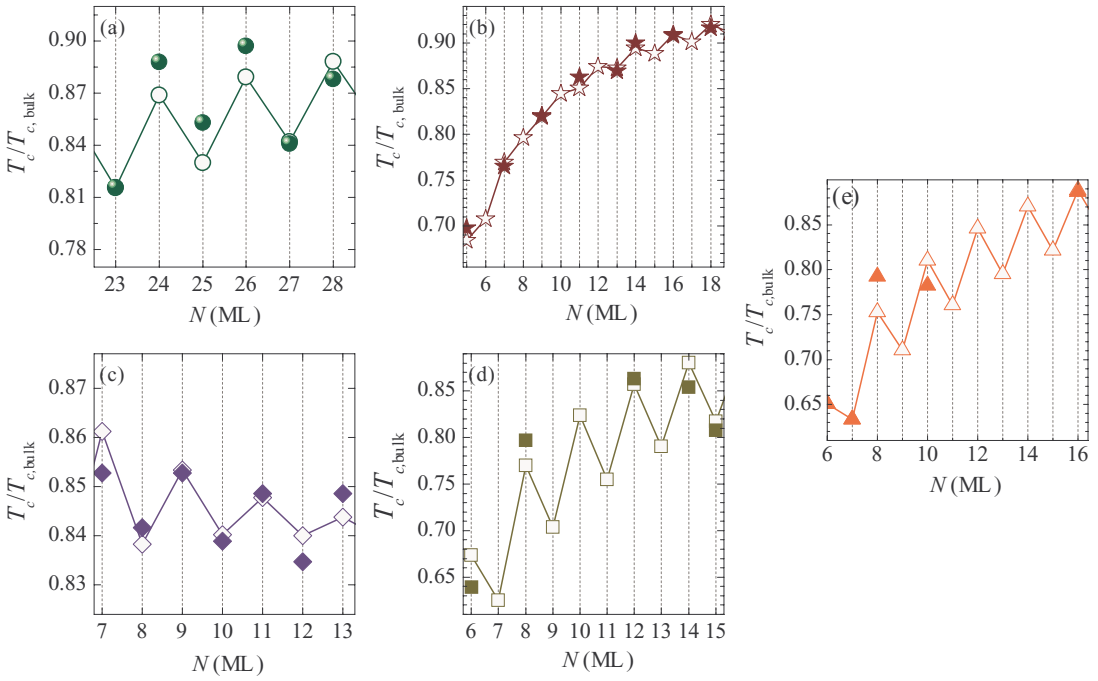

FIG. 2. (Color online) Theoretical results for the even-odd oscillations of T_c (open symbols) versus the experimental data (solid symbols): (a) Theoretical data were calculated for $g_1(\pi) = 1.67g_0$ (odd numbers) and $g_1(2\pi) = 2.13g_0$, and the experimental set is from Ref. 9; (b) theoretical data were calculated for $g_1(\pi) = 0.64g_0$ (odd) and $g_1(2\pi) = 1.46g_0$ (even), and experimental results are from Ref. 4; (c) the same as in the previous panels but for $g_1(\pi) = -0.12g_{\mathrm{eff}}$ and $g_1(2\pi) = 0.84g_{\mathrm{eff}}$ [where $g_{\mathrm{eff}}N_{\mathrm{bulk}}(0) = 0.36$], and the experimental set is from Ref. 5; (d) the same as in previous panels but for $g_1(\pi) = 1.08g_0$ and $g_1(2\pi) = 1.54g_0$, and the experimental set is from Ref. 9 [for the interface Si(111)$(7 \times 7) - $Pb]; (e) the theoretical data were calculated for $g_1(\pi) = 1.05g_0$ and $g_1(2\pi) = 1.59g_0$, and the experimental set is from Ref. 9 [for the interface Si(111)$(\sqrt{3} \times \sqrt{3}) - $Pb].

g_0. By choosing $g_{\mathrm{eff}}N_{\mathrm{bulk}}(0) = 0.36$, $g_1(\pi) = -0.12g_{\mathrm{eff}}$ and $g_1(2\pi) = 0.84g_{\mathrm{eff}}$, we compare our results (the open symbols) with the experimental critical temperature data (the solid symbols). As follows from Fig. 2(c), we again obtain very good agreement with the experimental data. As $g_1(\pi) < 0$, the total electron-phonon coupling constant $g_{\mathrm{eff}} - g_1/N$ for the odd-layered nanofilms is slightly above the effective-bulk value 0.36 and increases when decreasing N. This is totally different from our analysis of the previous data sets, and the direct consequence of this feature is that T_c does not show an overall decrease with decreasing nanofilm thickness. As seen, in this case the thickness-dependent oscillations of the electron-electron coupling "kills" such a decrease typical of the remaining experimental data sets. Note that the appearance of the positive interface-induced contribution to g for the odd-layered films, is not a surprise. For example, a similar effect was found for Ag films deposited on top of Fe(100) whisker.

Figures 2(d) and 2(e) show the comparison of our numerical data with data (the fourth and fifth sets, respectively) for T_c from Ref. 9. For Pb nanofilms grown epitaxially on Si(111)(7×7) [Fig. 2(d)] we performed calculations with the fitting parameters $g_1(\pi) = 1.08g_0$ and $g_1(2\pi) = 1.54g_0$. For films with interface Si(111)$(\sqrt{3} \times \sqrt{3}) - $Pb we used $g_1(\pi) = 1.05g_0$ and $g_1(2\pi) = 1.59g_0$. For the fourth set we focus on the range below the phase-slip point $N = 16$ ($N \leqslant 15$). For the fifth set we work above the phase-slip thickness $N = 6$ ($N \geqslant 7$). Here T_c increases for the even-layered nanofilms and decreases for the odd-layered ones for both data sets. However, similar to what was previously found for the first data set, the coupling $g_0 - g_1/N$ exhibits just the opposite size oscillations. As T_c follows the trend $\sim e^{1/(-gN(0))}$, one sees that the thickness-dependent oscillations of $N(0)$ are π shifted with respect to the oscillations of g, but the increase of $N(0)$ has a more significant effect than the corresponding decreases of g for an even number of monolayers. It is interesting to note that the fourth and fifth experimental data sets are characterized by almost the same coupling between electrons (the difference in g is less than 1%). So, for the experiments reported in Ref. 9, g is not sensitive to the change of Si(111) surface crystal ordering from (7×7) to $(\sqrt{3} \times \sqrt{3})$. Here the question arises why the results of Ref. 9 are so different with respect to those of Ref. 5. One possible reason may be the difference in the quality of the silicon substrate which may have a significant impact on the interface phonons, as seen from the completely different values of g_1 found from our analysis in Figs. 2(c) and 2(d).

Note that the first and second data sets in the present study were considered in our previous work.[2] However, in that paper we performed time-consuming calculations invoking the full BdG formalism. As already explained above [see the discussion after Eq. (9)], the full-BdG-based numerical procedure of determining the critical temperature often results in an overestimation of T_c that is larger than the errors of about a few percent induced by the Anderson approximation. This is the reason why in the present paper we have chosen to use the Anderson-approximation-based analysis of the available data, including the two data sets considered previously in Ref. 2.

We also note that we did not discuss error bars for the experimental data in the present paper because they do not influence our results qualitatively: The fitting parameters may be slightly different but the main conclusion about the crucial importance of the interplay of quantum-size oscillations of g and $N(0)$ will remain unaltered.

IV. CONCLUSIONS

We have analyzed five experimental data sets for the critical temperature of ultrathin Pb nanofilms deposited on top of Si(111). We have demonstrated that all these data sets can be reproduced within the BdG formalism. We addressed the important problem that the experimentally found amplitudes of the quantum-size oscillations of T_c vary significantly from one experiment to another. We showed that the reason for this difference is an interplay of the quantum-size variations in the single-electron density of states with the thickness-dependent oscillations in the phonon-mediated coupling between the electrons. Such oscillations of the coupling depend on the substrate material, the quality of the interface, the presence or absence of a protection cover and other fabrication details that change from one experiment to another. In addition, we demonstrated that oscillations in the coupling g and their interplay with the thickness-dependent variation of the density of states can even significantly change the overall trend of T_c with decreasing nanofilm thickness.

ACKNOWLEDGMENTS

This work was supported by the Flemish Science Foundation (FWO-Vl).

*francois.peeters@ua.ac.be

[1] J. M. Blatt and C. J. Thompson, Phys. Rev. Lett. **10**, 332 (1963).
[2] A. A. Shanenko, M. D. Croitoru, and F. M. Peeters, Phys. Rev. B **75**, 014519 (2007).
[3] Y. Guo, Y.-F. Zhang, X.-Y. Bao, T.-Z. Han, Z. Tang, L.-X. Zhang, W.-G. Zhu, E. G. Wang, Q. Niu. Z. Q. Qiu, J.-F. Jia, Z.-X. Zhao, and Q.-K. Xue, Science **306**, 1915 (2004).
[4] M. M. Özer, J. R. Thompson, and H. H. Weitering, Nat. Phys. **2**, 173 (2006).
[5] D. Eom, S. Qin, M.-Y. Chou, and C. K. Shih, Phys. Rev. Lett. **96**, 027005 (2006).
[6] M. M. Özer, Y. Jia, Z. Zhuang, J. R. Thompson, and H. H. Weitering, Science **316**, 1594 (2007).
[7] J. J. Paggel, T. Miller, and T.-C. Chiang, Science **12**, 1709 (1999).
[8] S. Qin, J. Kim, Q. Niu, and C.-K. Shih, Science **324**, 1314 (2009).
[9] C. Brun, I. Po Hong, F. Patthey, I. Y. Sklyadneva, R. Heid, P. M. Echenique, K. P. Bohnen, E. V. Chulkov, and W.-D. Schneider, Phys. Rev. Lett. **102**, 207002 (2009).
[10] T. Zhang, P. Cheng, W.-J. Li, Y.-J. Sun, G. Wang, X.-G. Zhu, K. He, L. Wang, X. Ma, X. Chen, Y. Wang, Y. Liu, H.-Q. Lin, J.-F. Jia, and Q.-K. Xue, Nat. Phys. **6**, 104 (2010).
[11] D.-A. Luh, T. Miller, J. J. Paggel, and T.-C. Chiang, Phys. Rev. Lett. **88**, 256802 (2002).
[12] C. M. Wei and M. Y. Chou, Phys. Rev. B **66**, 233408 (2002).
[13] Y.-F. Zhang, J.-F. Jia, T.-Z. Han, Z. Tang, Q.-T. Shen, Y. Guo, Z. Q. Qiu, and Q.-K. Xue, Phys. Rev. Lett. **95**, 096802 (2005).
[14] J. Noffsinger and M. L. Cohen, Phys. Rev. B **81**, 214519 (2010).
[15] Y. Chen, A. A. Shanenko, and F. M. Peeters, Phys. Rev. B **81**, 134523 (2010).
[16] P. G. de Gennes, *Superconductivity of Metals and Alloys* (Benjamin, New York, 1966).
[17] A. L. Fetter and J. D. Walecka, *Quantum Theory of Many-Particle Systems* (Dover, Mineola, 2003).
[18] D. G. Naugle, J. W. Baker, and R. E. Allen, Phys. Rev. B **7**, 3028 (1973).